AIP Applied Physics Letters

Antenna configuration for uniform large-area inductively coupled plasma production

S. S. Kim, H. Y. Chang, C. S. Chang, and N. S. Yoon

Citation: Appl. Phys. Lett. **77**, 492 (2000); doi: 10.1063/1.127021
View online: http://dx.doi.org/10.1063/1.127021
View Table of Contents: http://apl.aip.org/resource/1/APPLAB/v77/i4
Published by the American Institute of Physics.

Additional information on Appl. Phys. Lett.

Journal Homepage: http://apl.aip.org/
Journal Information: http://apl.aip.org/about/about_the_journal
Top downloads: http://apl.aip.org/features/most_downloaded
Information for Authors: http://apl.aip.org/authors

ADVERTISEMENT

Downloaded 18 Apr 2013 to 143.248.118.122. This article is copyrighted as indicated in the abstract. Reuse of AIP content is subject to the terms at: http://apl.aip.org/about/rights_and_permissions

Antenna configuration for uniform large-area inductively coupled plasma production

S. S. Kim,[a] H. Y. Chang, and C. S. Chang
Department of Physics, Korea Advanced Institute of Science and Technology, Taejon, Korea 305-701

N. S. Yoon
School of Electrical and Electronics Engineering, Chungbuk National University, Cheongju, Korea 361-480

(Received 10 March 2000; accepted for publication 31 May 2000)

An antenna configuration for uniform plasma generation in a large-area inductively coupled plasma (ICP) source is presented and investigated using numerical analysis. The numerical results show that a properly tuned, segmented coil system with an external variable capacitor can allow antenna voltage, currents, and plasma uniformity to be controlled in the large-area ICP source. The key element of this concept is to induce LC-resonance in the coil system by the external capacitance variation. Through the LC-resonance, not only a small antenna voltage can be obtained, but also a selected coil current near a low plasma density regime can be significantly enhanced. Self-consistent fluid simulations for Ar and Cl_2 plasmas indicate that the radial plasma spread can be optimized near the LC-resonance condition. © *2000 American Institute of Physics.* [S0003-6951(00)04830-0]

In microelectronic and flat panel display device fabrication, the development of a uniform high-density plasma source with a large area is of major concern. Particularly, in the ultralarge scale integrated-circuit etching process, the development of plasma process devices to handle larger area wafers is needed urgently as the current 200 mm wafer diameter is projected to increase to 300 mm by the year 2001.[1] Recently, there have been efforts to generate uniform high-density plasmas over a large area by various discharge methods, such as inductively coupled discharge using multiple inductive elements operated in parallel,[2] modified magnetron-typed radio frequency (rf) discharge,[3] or ultrahigh-frequency discharge using a spokewise antenna.[4] In this letter, we present a modified inductively coupled plasma (ICP) source with a new antenna configuration for the next generation large-area wafer processing.

The ICP source has been a popular choice for the current wafer processing due to its geometric simplicity and ability to produce uniform plasma at high density without relying upon external magnetic coils.[5–8] However, a conventional ICP source using a multiturn spiral coil antenna has reached its limit in extending the process area due to its large inductance, which causes large voltage between the ends of the antenna and unstable impedance matching. The large voltage can lead the antenna to be capacitively coupled with the plasma causing a low efficiency and nonuniform plasma production.

Our antenna coil system is designed to overcome the large inductance problem and further to control coil current distribution. It is described schematically in Fig. 1(a): a six-turn coil is segmented and the segments are connected in parallel. The connection of the coil segments in parallel allow the inductance of the present antenna system to be very small as compared with that of the six-turn spiral antenna: calculated inductance values under our geometric configuration are $\omega L_{\mathrm{spiral}} \simeq 605\ \Omega$ for the spiral case and $\omega L_{\mathrm{seg}} \simeq 8\ \Omega$ for the segmented case at 13.56 MHz rf, respectively. However, this coil segmentation makes the inner coils have small inductance as compared with the outer coils and accordingly induces large inner coil currents causing a radially nonuniform plasma. To overcome this problem, one of the segmented coils is connected with an external variable capacitor in series [see the most outer coil in Fig. 1(a)]. Through numerical simulation, it will be shown that this variable capacitor serves as an external parameter for the antenna current distribution and plasma uniformity control.

To determine the coil currents from the processing parameters and the external variable capacitance, we have used an equivalent circuit model. The equivalent circuit diagram to this system is presented in Fig. 1(b). In Fig. 1(b), Z_j ($j=1-6$) denotes lumped impedance of the jth coil with plasma and Z_v is the impedance of the variable capacitor. $I_A = \Sigma_{j=1}^{5} I_j$, where I_j is the jth coil current, and $I_B = I_6$ are currents into circuit elements A and B, respectively. Here the circuit element B contains the coil which is connected with the variable capacitor in series and the element A contains the other coils. The key technique of this concept is to adjust the reactance of the circuit element B to the reactance of the element A with the external capacitance variation and to form a parallel LC-resonant circuit. As will be shown, this induces LC resonance in the circuit C which is the series connection of the circuit element A with B. At the resonance condition, the current from B becomes nearly the same as the current into A. As a result, antenna currents can be concentrated on the coil which is connected with the variable capacitor in series. Choice of the current-concentrated coil is closely related to the plasma uniformity. To control the plasma uniformity, the coil should be chosen as one located near a relatively low plasma density regime. In this case, it was chosen as the sixth coil from the center.

To resolve the equivalent circuit system, we have used a recently developed analytic model for a planar type ICP

[a]Electronic mail: sskim@comp.kbsi.re.kr

Downloaded 18 Apr 2013 to 143.248.118.122. This article is copyrighted as indicated in the abstract. Reuse of AIP content is subject to the terms at: http://apl.aip.org/about/rights_and_permissions

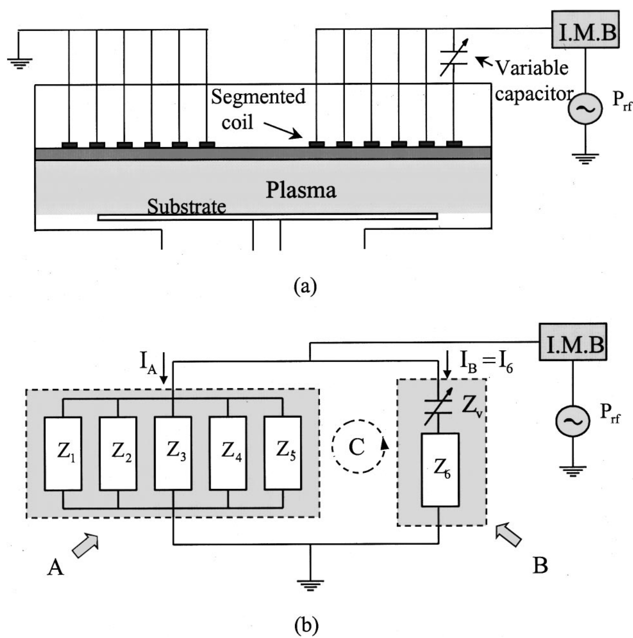

FIG. 1. Schematic diagram of (a) a large-area ICP source with antenna composed of segmented coils and an external variable capacitor and (b) its equivalent circuit.

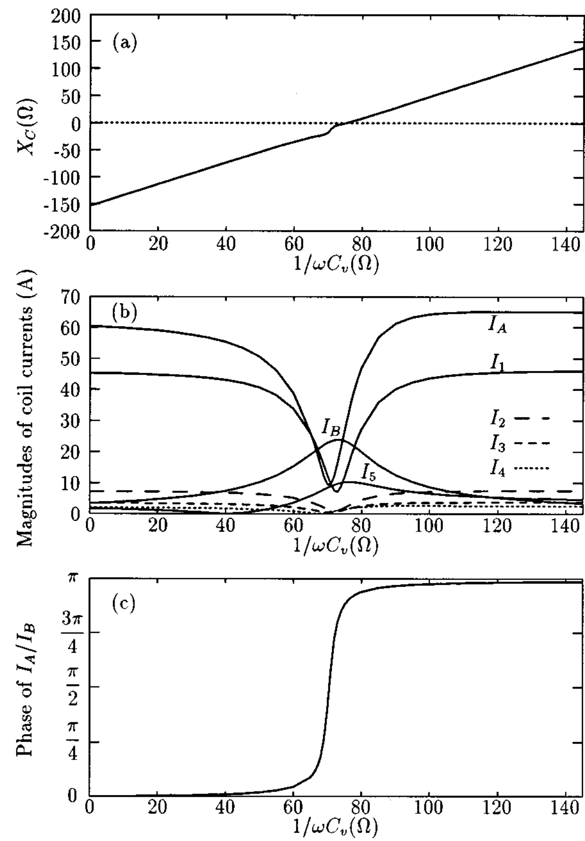

FIG. 2. Dependence of (a) reactance of the circuit C in Fig. 1(b), (b) magnitudes of the coil currents, and (c) phase difference between I_A and I_B on the reactance of the external variable capacitor under Ar discharge condition of 500 W rf power and 10 mTorr gas pressure.

heating and impedance formula, including a collisionless nonlocal election heating mechanism.[9–11] Using the analytic results in Refs. 9–11 and the complex Poynting theorem,[12] we can obtain the coil currents and voltage. The obtained coil currents are used in calculating the Fourier–Bessel series solution of the inductive field[10,11] and plasma power deposition.

To determine the plasma density and electron temperature in a self-consistent manner, we have performed two-dimensional fluid simulations. We used the implicit finite difference method on staggered uniform grids in solving the fluid equations. To avoid the restriction on the size of the spatial grids,[13] the exponential scheme for continuity equations[14] was used. To overcome the dielectric relaxation time restriction on the maximum time step size,[7] we used a semi-implicit numerical scheme. In this scheme, the electrostatic field is evolved so that the net plasma current density induced at the previous time step decays exponentially within the dielectric relaxation time. Details of the numerical scheme will be presented elsewhere.

Simulation results were obtained for Ar and Cl_2 discharges under 10 mTorr pressure and 500 W rf-power condition: Ar is a commonly used gas in investigating the device characteristics and Cl_2 is a widely used etchant in polycrystalline silicon etching. The used geometric parameters are as follows: the chamber radius is 30 cm, the chamber length is 15 cm, the shielding cap length is 15 cm, the thickness of the dielectric window is 2 cm, the substrate radius is 25 cm, the coil thickness and width are 0.2 and 2 cm, respectively, and the coils are spaced at 4, 8, 12, 16, 20, and 24 cm apart from the center, respectively.

Figure 2 shows the circuit variable results for Ar discharges. Figure 2(a) presents the dependence of the reactance of the circuit C, $X_C = X_A + X_B$, on the magnitude of $Z_v = i/\omega C_v$, where X_A and X_B are the reactances of the circuit element A and B, respectively, and C_v is the variable capacitance. Figure 2(b) shows variations of the coil current magnitudes with the external capacitance variation. Figure 2(c) shows the phase difference between I_A and I_B. As can be seen from Figs. 2(a), 2(b), and 2(c), LC-resonance phenomena occurs in the circuit C near $X_C = 0$: the magnitudes of $I_A = \Sigma_{j=1}^{5} I_j$ and $I_B = I_6$ become nearly the same with each other, but their directions become opposite. As a result, a resonance peak appears in the sixth coil current magnitude at $1/\omega C_v = 73\,\Omega$. Since the increase of the sixth coil current means the increase of the plasma generation in the radially outer region, we can easily expect that the radial plasma spread may be controlled and optimized at a proper C_v value.

Figure 3 shows the dependence of the antenna terminal voltage V on the reactance of the variable capacitor under the same discharge condition with that of Fig. 2. Since at the resonance condition the current directions of I_A and I_B become opposite to each other but their magnitudes become nearly the same, the input antenna current $I = I_A + I_B$ becomes very small. The decrease of the input antenna current I makes the antenna voltage V very small near the resonance condition, as shown in Fig. 3.

Figure 4 presents the fluid simulation results for the radial plasma density profiles of the Ar plasma at substrate position with various C_v. The external capacitances for off-resonance cases yield centrally peaked density profiles. However, as C_v goes to values near the resonance point, the radial density profile becomes uniform. When $1/\omega C_v = 68\,\Omega$, the radial spread of the plasma is optimized and uniform

Downloaded 18 Apr 2013 to 143.248.118.122. This article is copyrighted as indicated in the abstract. Reuse of AIP content is subject to the terms at: http://apl.aip.org/about/rights_and_permissions

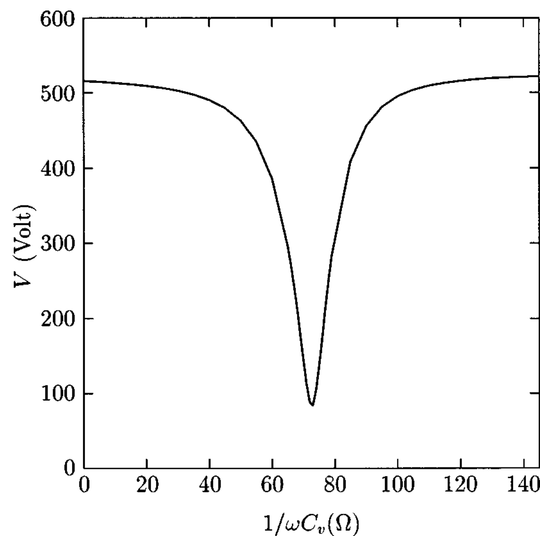

FIG. 3. Dependence of terminal voltage of the antenna coil on the reactance of the external variable capacitor under Ar discharge condition of 500 W rf power and 10 mTorr gas pressure.

within 2% over 300 mm in diameter. The coil current distribution at the resonance peak point, $1/\omega C_v = 73\,\Omega$, yields a slightly hollow density profile.

The Cl_2 plasma results for the antenna current distribution and voltage, which is not presented here, show nearly the same dependence on the variable capacitance as the Ar plasma case, except for the slightly shifted resonance peak position. Figure 5 presents the radial profile results for total ion flux of Cl_2 plasma, which is the sum of Cl^+ and Cl_2^+ ion fluxes, at the substrate position with various C_v. Here we plotted ion flux instead of density because in the ion enhanced silicon etching process by Cl_2 plasma, the silicon etch rate is proportional to the total ion flux.[15] As shown in Fig. 5, the dependence of the total ion flux profiles on C_v is nearly same as the Ar plasma density profile dependence: it shows centrally peaked profiles for off-resonance cases and a slightly hollow profile at the resonance point $1/\omega C_v = 77\,\Omega$. The optimum ion flux profile with uniformity of 2.4% over 300 mm in diameter is obtained at $1/\omega C_v = 70\,\Omega$.

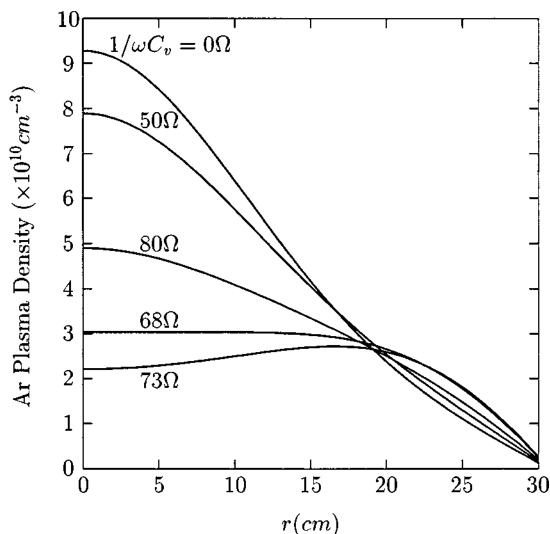

FIG. 4. Radial profiles of the Ar plasma density on the substrate with various external capacitance when rf power is 500 W and pressure is 10 mTorr.

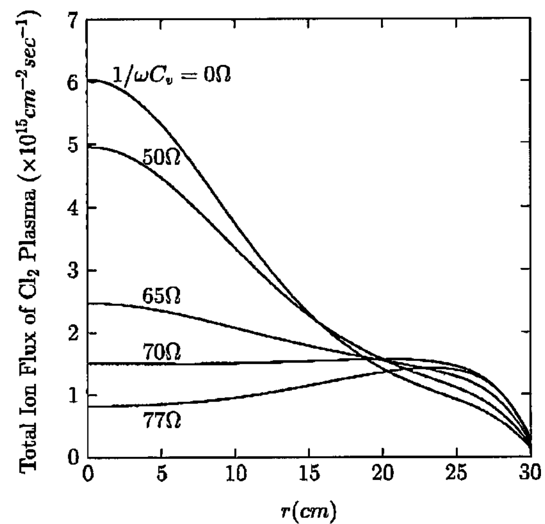

FIG. 5. Radial profiles of the total ion flux of Cl_2 plasma on the substrate with various external capacitance when rf power is 500 W and pressure is 10 mTorr.

In summary, through numerical study it is found that a properly tuned six-segmented coil system with an external variable capacitor can not only diminish antenna voltage but also produce a uniform large-area ICP. The numerical results indicate that the small antenna voltage and the uniform plasma density are caused by LC resonance in the coil system induced by the external capacitance variation. Even though the present study is carried out for only a six-segmented coil system, the scheme could be applicable to any number of coil segments. This scheme could be applied to antenna design for 300 mm wafer processing with a large-area ICP device.

The authors gratefully acknowledge useful discussions with Dr. P. W. Lee. This work is supported by the Korea Ministry of Science and Technology and the Korea Ministry of Commerce, Industry and Energy under System IC project contract.

[1] D. J. Economou and T. J. Bartel, IEEE Trans. Plasma Sci. **24**, 131 (1996).
[2] V. Singh and J. Holland, IEEE Trans. Plasma Sci. **24**, 133 (1996).
[3] Y. Li, S. Iizuka, and N. Sato, Appl. Phys. Lett. **65**, 28 (1994).
[4] S. Samukawa, Y. Nakagawa, T. Tsukada, H. Ueyama, and K. Shinohara, Appl. Phys. Lett. **67**, 1414 (1995).
[5] J. Hopwood, C. R. Guarnier, S. J. Whitehair, and J. J. Cuomo, J. Vac. Sci. Technol. A **11**, 152 (1993).
[6] M. S. Barnes, J. C. Foster, and J. H. Keller, Appl. Phys. Lett. **62**, 2622 (1993).
[7] P. L. G. Ventzek, T. J. Sommerer, R. J. Hoekstra, and M. J. Kushner, Appl. Phys. Lett. **63**, 605 (1993).
[8] M. A. Liebermann and A. J. Lichtenberg, *Principles of Plasma Discharges and Materials Processing* (Wiley, New York, 1994).
[9] N. S. Yoon, S. S. Kim, C. S. Chang, and D. I. Choi, Phys. Rev. E **54**, 757 (1996).
[10] N. S. Yoon, S. M. Hwang, and D. I. Choi, Phys. Rev. E **55**, 7536 (1997).
[11] N. S. Yoon and S. S. Kim (unpublished).
[12] J. D. Jackson, *Classical Electrodynamics* (Wiley, New York, 1975).
[13] Y. H. Oh, N. H. Choi, and D. I. Choi, J. Appl. Phys. **67**, 3264 (1990).
[14] S. V. Patankar, *Numerical Heat Transfer and Fluid Flow* (McGraw-Hill, New York, 1980).
[15] M. Tuda, K. Nishikawa, and K. Ono, J. Appl. Phys. **81**, 960 (1997).

Downloaded 18 Apr 2013 to 143.248.118.122. This article is copyrighted as indicated in the abstract. Reuse of AIP content is subject to the terms at: http://apl.aip.org/about/rights_and_permissions